

## Web shear buckling capacity of a stiffened Z-purlin: reporting of experimental tests

Almir Benedito<sup>1</sup>, Diego Fernandes<sup>1</sup>, Guilherme S. Alencar<sup>1</sup>, José Luís Vital de Brito<sup>1</sup>

<sup>1</sup> *Postgraduate Program in Structures and Civil Construction (PECC), University of Brasilia (UnB).  
Campus Universitário Darcy Ribeiro, s/n, Asa Norte, 70910-900, Brasília-DF, Brazil.  
Corresponding author: almir.benedito@outlook.com*

**Abstract.** Over the last few years there was a growing demand for structural solutions with lower steel consumption in the design of portal frames. It is considered that cold-formed steel (CFS) represents a consumption of 30 to 40% of steel in the entire structure, due to its great applicability in roof systems. Purlins with Z-sections have capabilities to achieve greater spans than other sections due to the continuity provided by overlapping connections. Greater spans require higher sections, thus increasing the susceptibility to local buckling of the web when the purlin is subjected to bending. Therefore, there is the need to introduce web stiffeners with complex geometry, providing better structural performance to local buckling strength. However, this also introduces complex web behaviour in the presence of shear, as result it requires advanced analytical, experimental and numerical studies to assess the web shear buckling mode of failure of such sections. In this context, as a first incursion in this field, the authors report in this paper some experimental tests of a new stiffened web cold-formed Z-section in the Brazilian market aiming the web shear buckling mode of failure. Consequently, experimental setups of simply supported beams with short spans under 3-point bending are carried out, combining both bending and shear. The flanges were locked to investigate the structural behaviour of CFS under predominantly shear. In the current stage of the present work, the experimental resistances are contrasted with shear capacity as prescribed in the AISI S100 [1] for an equivalent plain-web Z-section (same overall geometry but without web stiffeners). Since this work is in the context of a dissertation under development at the University of Brasília, in a later stage the experimental results will be compared with the actual Z-section with web stiffeners, which will require an elastic shear buckling analysis with the aid of the finite element method to determine critical buckling elastic shear stresses. The results were evaluated providing a better understanding of the structural behaviour of the CFS Z-sections with stiffened webs.

**Keywords:** Cold-formed sections, High strength steel, Shear buckling. Combined bending and shear, Direct strength method

## 1 Introduction

Cold-formed steel (CFS) is produced in roll-forming machines or by press brake or bending brake operations. The thickness of steel sheets or strip ranging from 0.4 mm to 25.5 mm. The simplicity of their production allows for a wide range of applications, including the automotive industry, aerospace industry, heavy transportation, agro-industries, and civil construction. When compared to hot-rolled shapes, several advantages of CFS are evident, such versatile cross-sectional configurations, ease of production, and low storage costs [2].

In roof purlins of industrial building, zed shapes are one of the most common CFS sectional profiles. The development of members with complex geometry cross-sections has been led because the growing demand for even more economical and versatile structures and the manufacture of high strength steel results in reduction of

thicknesses. The most common types of profiles can be observed in the image below [3], Figure 1.

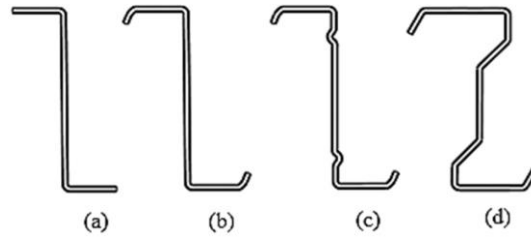


Figure 1. Types of geometry of cross section of CFS purlins [4].

Purlins with Z-sections have capabilities to achieve greater spans than other sections due to the continuity provided by overlapping connections. Greater spans require higher sections, thus increasing the susceptibility to local buckling of the web when the purlin is subjected to bending. Therefore, there is the need to introduce web stiffeners with complex geometry, providing better structural performance to local buckling strength. However, this also introduces complex web behaviour in the presence of shear, as result it requires advanced analytical, experimental and numerical studies to assess the web shear buckling mode of failure of such sections. In this context, as a first incursion in this field, the authors report in this paper some experimental tests of a new stiffened web cold-formed Z-section in the Brazilian market, with the shape similar to Figure 1d with corrugated longitudinal web stiffeners, aiming the web shear buckling mode of failure.

## 2 Cold Formed Steel Design to Web Shear Buckling according to AISI

Buckling due to shear in the web is a crucial phenomenon in the design of cold-formed steel purlins. This failure is predicted by provisions available in the standard AISI S100-16 (North American Specification for the Design of Cold-Formed Steel Structural Members). The shear buckling occurs when a shear force applied in the beam causes instability in the cross-section. According AISI, the elastic shear buckling stress ( $F_{cr}$ ) and the shear buckling force of a web ( $V_{cr}$ ) are given for equation 1 and 2, respectively.

$$F_{cr} = \frac{\pi^2 E k_v}{12(1 - \nu^2)(h/t)^2} \quad (1)$$

$$V_{cr} = A_w F_{cr} \quad (2)$$

Where  $E$  = young's modulus,  $k_v$  = shear buckling coefficient,  $\nu$  = poisson's ratio,  $h$  = web height,  $t$  = web thickness and  $A_w$  = area of web element.

The nominal shear strength,  $V_n$ , of a cold-formed steel member is determined using the previous shear buckling force and the dimensions of the web.

$$V_n = V_y \text{ for } \lambda_v \leq 0.815 \quad (3)$$

$$V_n = 0.815 \sqrt{V_{cr} V_y} \text{ for } 0.815 \leq \lambda_v \leq 1.227 \quad (4)$$

$$V_n = V_{cr} \text{ for } \lambda_v > 1.227 \quad (5)$$

Where  $\lambda_v = \sqrt{V_y/V_{cr}}$ ,  $V_n$  = nominal shear strength,  $V_y$  = yield shear force of cross-section. The yield shear force of cross-section is given by  $V_y = 0.6 A_w f_y$ ,  $f_y$  = yield stress.

Conducting a pure shear test on cold-formed steel elements poses significant challenges due to the complexity of accurately applying and measuring shear forces. As a result, the analysis of shear resistance must be supplemented by evaluating the flexural strength of the element according to AISI S100-16. In this context, the nominal flexural strength ( $M_n$ ) must be determined to ensure the element can withstand the applied loads. The elastic critical moment can be determined by the Finite Strip Method, which can be determined with the aid of software such as CUFSM [5].

For beams subject to combined bending and shear, it must be considered the interaction between bending moment and shear. It's very important to consider both shear and bending because of the interaction of the effects. According to AISI S100-16, for beams without transverse shear stiffeners, the moment due to factored loads,  $\bar{M}$ , and the shear force due to factored loads,  $\bar{V}$ , shall also to satisfy the interaction equation:

$$\sqrt{\left(\frac{\bar{M}}{M_{alo}}\right)^2 + \left(\frac{\bar{V}}{V_a}\right)^2} \leq 1.0 \quad (6)$$

Where  $M_{alo}$  is factored flexural resistance and  $V_a$  is the factored shear resistance. The Equation is understood to be used in the context of Cold Formed Design of steel structures with the aid of the Load and Resistance Factor Design (LRFD). On the other hand, when dealing with experimental results, this Equation shall be used without factored coefficients applied to the nominal loads and resistances values.

### 3 Experimental setup

The test program included four cold-formed steel (CFS) beams with different web cross-sections and different thicknesses. The tests were performed to achieve predominantly shear to specimens, although the bending influence cannot be excluded. The design of the test rig was based on works developed by LaBoube and Yu [6] and Pham and Hancock [7]. The test setup consists of simply supported beams with supports at both ends, creating a clear span between them. A concentrated load is applied at the beams mid span, which maximizes the shear forces in the beams. The shear span was defined as the distance between the lines of bolts at the loading and support points. The beams were tested in pairs with their bottom flanges facing inwards to prevent lateral buckling and were braced at the top with angle sections to prevent distortional buckling (Figure 2).

The instrumentation utilized in this study involved the application of displacement transducers for measuring displacement, a load cell at the mid span to measure the applied force and strain gauges for measuring strains. Two displacement transducers were positioned at the mid-span of the beams, one sensor at each beam. A C50T load cell from *Alfa Instrumentos Ltda.* was used for load measurement. To verify the stresses in the profile section, triaxial strain gauges (rosettes) were employed and positioned on the web at 1/4 of the theoretical span. Data acquisition was performed using a Lynx ADS-2000 system, equipped with two AI2161 modules with each one containing 16 channels.

Through Table 1 and Figure 3a, it is possible to observe the various dimensions used in the tests. For comparison purposes, the experimental shear strengths will be contrasted with an equivalent plain-web Z-section (Figure 3b), with the overall dimensions of the web stiffened Z-section, but without web stiffeners. The suitable approach to assess the shear strength of the Z-section with web stiffeners with accuracy requires an advanced numerical analysis with the aid of the Finite Element Method to obtain shear buckling critical elastic stresses, as recommended by Appendix 2 of AISI S100-16. This will be done in a later stage of the current dissertation thesis under development at University of Brasília. Thus, in this first stage, just for comparison purposes, the experimental shear strengths will be compared with a Z-section with plain web, which is a well-documented section in both literature and standards (classified as pre-qualified section as per the AISI S100-16).

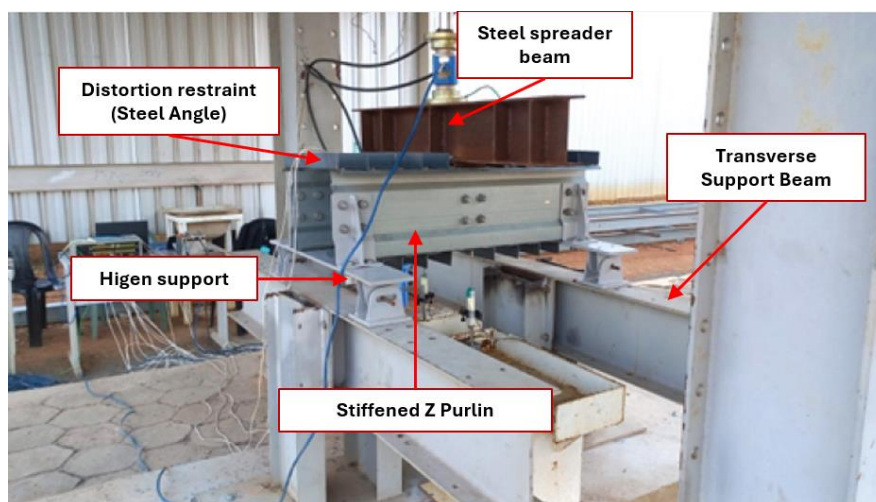


Figure 2. Experimental setup: three-point bending test.

Table 1. Dimensions.

Dimensions of the Z-section with web stiffeners (actual tested specimens)										
Specimen	Z	h <sub>1</sub>	h <sub>2</sub>	h <sub>3</sub>	b <sub>1</sub>	b <sub>2</sub>	e <sub>1</sub>	e <sub>2</sub>	da <sub>1</sub>	da <sub>2</sub>
Specimen 1	204.00	38.00	46.00	81.00	75.00	82.00	16.00	16.00	29.50	29.50
Specimen 2	500.00	71.00	79.00	310.00	98.00	105.00	23.00	23.00	29.50	29.50
Specimen 3	300.00	53.00	55.00	148.00	82.00	89.00	19.00	19.00	21.00	21.00

Dimensions of an equivalent Zed with plain web (for contrasting purpose)			
Specimen	Z	b	e
Z-200-2.70-ST	200	73	21
Z-300-1.25-ST	300	82	19
Z-500-2.70-ST	500	99	16

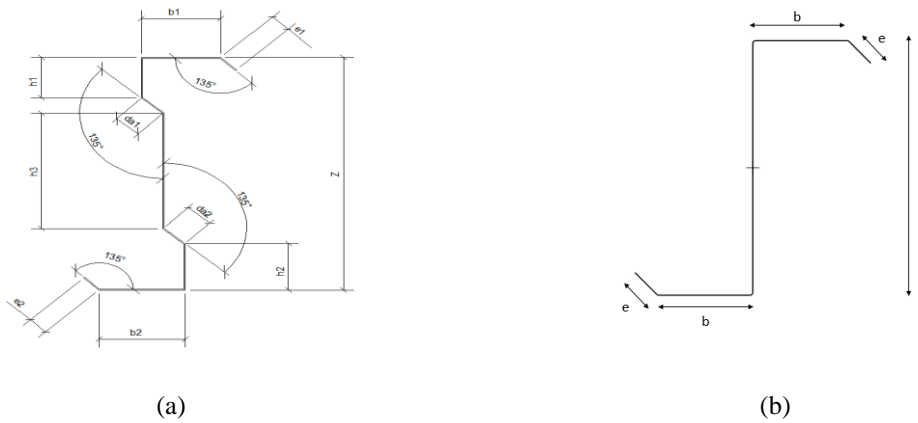


Figure 3. Symbol definition of Z section with longitudinal corrugated web stiffeners and plan web zed section

The steel commonly used in Cold-Formed Steel (CFS) in Brazilian market is high-strength galvanized ZAR steel [8], coated with zinc through a continuous hot-dip process, providing excellent corrosion resistance and increased durability. Due to the nonlinear analysis, it is crucial to clearly define the three phases (elastic, yield, and post-rupture strain hardening) in the Stress-Strain diagram. The specific type of steel is ZAR 400, with a nominal strength of 400 MPa. Tensile tests were conducted according to ASTM A370 standards [9] enabling precise plotting of the Stress-Strain curve as show in Figure 4. The obtained results were  $E= 194 \text{ GPa}$  and  $f_{yk} = 470 \text{ MPa}$ .

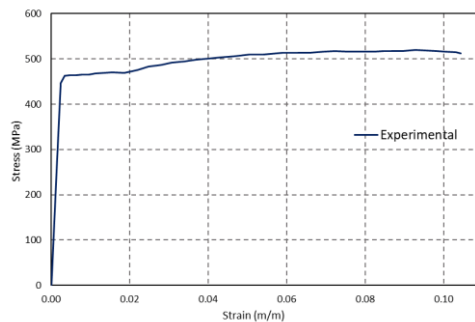


Figure 4. Static stress-strain curves [4].

## 4 Results and discussion

### 4.1 Experimental results

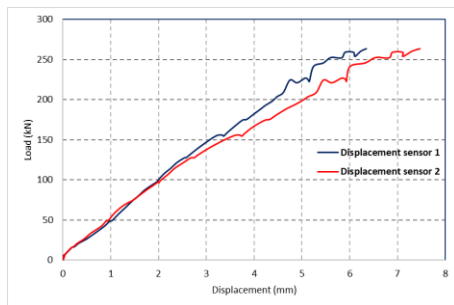
Since each specimen has two beams, the load on each beam is assumed as half of the experimental force. Table 2

presents a summarized view of the results obtained from the experimental tests, including maximum load and maximum displacements at the instant of maximum load, as well as providing specifications for the beam, such as thickness and material.

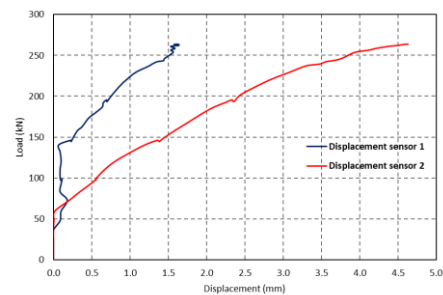
Table 2. Specifications and Experimental Results.

Specifications				
Height	Nominal Thickness	Material	Max. Load + Dead Load (kN)	Maximum Displacement at the Maximum Load (mm)
200	2.70	ZAR-400	269.7858	7.47
200	2.70	ZAR-400	269.8858	4.63
300	1.25	ZAR-400	106.7358	4.40
500	1.70	ZAR-400	202.8059	6.55
500	1.70	ZAR-400	203.5559	6.35

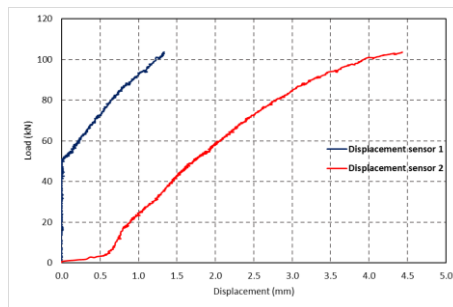
The following graphs illustrate the relationship between force and displacement obtained from the experimental tests. Each curve represents the structural response of the beams under loading until failure as show in Figure 5. The data were collected for different thickness and material configurations, as specified in Table 2.



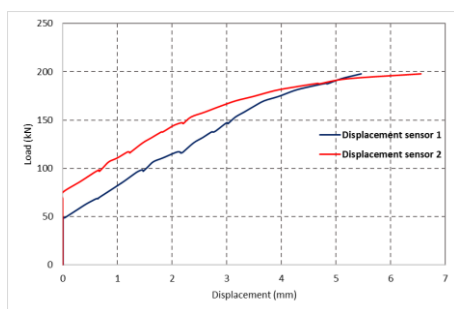
a) ZPRO-200-2.70-ST#1



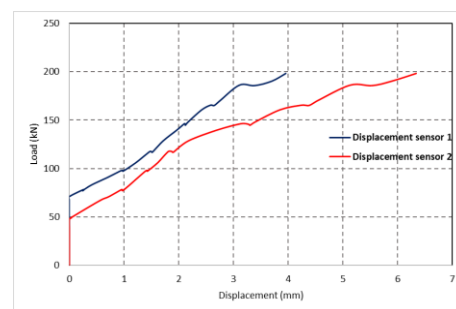
b) ZPRO-200-2.70-ST#2



c) ZPRO-300-1.25-ST#1



d) ZPRO-500-1.70-ST#1



e) ZPRO-500-1.70-ST#2

Figure 5. Load vs. Displacement Experimental Results.

The following Figure 6 depict the shear failures of beams with heights of (a) ZPRO-500-1.70-ST#2 and (b) ZPRO-300-1.25-ST#1. In the following, the ZPRO-300-1.25-ST#1 purlin is equipped with rosette strain gauges. Due to higher loads, the tested sections with 500 mm height, a special and stiffer purlin support was designed (as can be seen in Figure 6a).

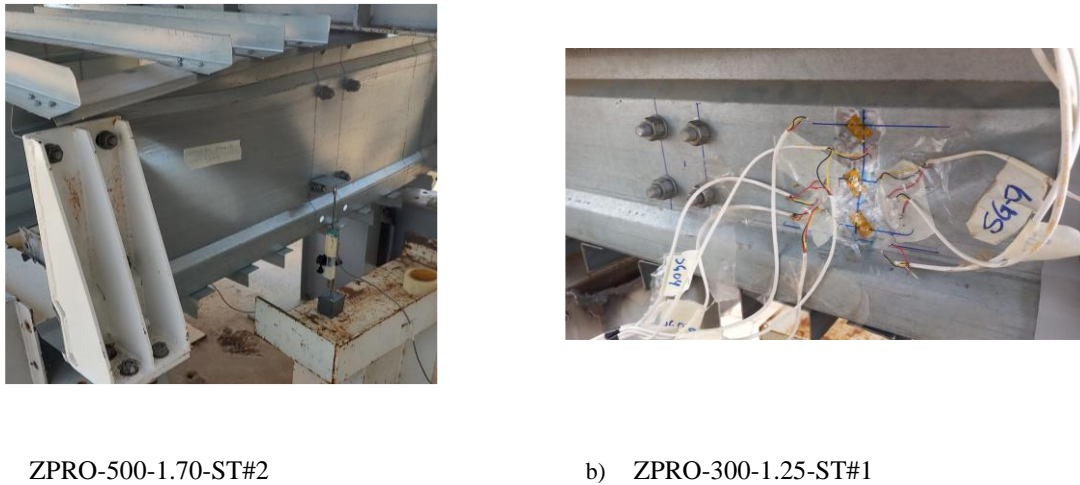


Figure 6. Failure modes in predominantly shear tests.

#### 4.2 Contrasting experimental results with nominal resistances of a plain web Z-section

The data provided in the following spreadsheets encompass critical measurements for structural analysis, including moments, shear forces, and the relationships between experimental and analytical values calculated using the Direct Strength Method for the bending moment capacities and the provisions for shear strength available in the AISI S100-16 for plain web zed. It is important to note that the analytical value to  $V_n$  shown in Table 4 was obtained considering a flat web section, since the plain web zed is a well-documented cold formed steel section and is also classified as a pre-qualified section according to AISI S100-16, just for contrasting purposes with the stiffened web and tested Z-sections. On the other hand, the  $M_{nd}$  (nominal bending resistance to distortional buckling) was obtained considering the actual tested Z-sections with web stiffeners using the Direct Strength Method.  $M_{exp}$  exhibits the acting bending moment at the section of shear failure (at  $\frac{1}{4}$  of the span) in the instant of maximum shear force in the web,  $V_{exp}$ . It is important to highlight that the maximum analytical nominal shear strength shown in Table 4 for plain web zed do not consider the shear and bending interaction Equation, that is, these shear strengths could only be theoretically achieved in the absence of any bending moment (which is a theoretical situation). The results of both Tables 3 and 4 were computed considering a nominal yield strength of 400 MPa (ZAR 400). Moreover, in Table 4,  $M_{nl}$  refers to the maximum nominal bending capacity to local buckling, since the equivalent plain web zed (with same overall geometry but without stiffeners) tends to fail to local buckling instead of distortional buckling.

Table 3. Experimental results and analytical analyses to

Specimen	$M_{nd}$ (kNm)	$M_{exp}$ (kNm) – Bending moment at $\frac{1}{4}$ span at maximum shear force	$V_n$	$V_{exp}$ (kN)
ZPRO-200-2.70-ST#1	25.63	11.52	To be computed in later stages of the present research <sup>1</sup>	65.88
ZPRO-200-2.70-ST#2	25.63	11.53		65.90
ZPRO-300-1.25-ST#1	14	4.53		25.91
ZPRO-500-1.70-ST#1	43.78	18.51		49.36
ZPRO-500-1.70-ST#2	43.78	18.57		49.54

<sup>1</sup> The computation of the nominal shear strength of the zed with stiffened web requires an elastic requires an elastic buckling analysis with the aid of FE method according to Appendix 2 of AISI S100-16.

Table 4. Results the analytical value considering a flat web section.

Specimen	$M_{nl}$ (kNm)	$V_n$ (kN)
Z-200-2.70-ST	22.47	89.43
Z-300-1.25-ST	9.21	5.42
Z-500-2.70-ST	22.60	8.30

For contrasting purposes, one can note that the effect of adding stiffeners in the web increased the overall resistance to shear strength, consistently exceeding the analytical values ( $V_n$ ), which were calculated based on flat webs. Of course, this was an expected result. In later stages of the present research, the actual analytical resistance of the stiffened web zed will be computed with the aid of FE analyses to obtain the shear elastic buckling critical stress, as recommended by Appendix 2 of AISI for sections not documented in the standard, as the studied in the present research. The present contrast of overall shear resistances between both sections, highlights the crucial role of web stiffeners in improving the load-carrying capacity under shear.

## 5 Conclusions

In conclusion, this work is a recent and promising study on the shear buckling capacity of stiffened Z-purlins. It has been observed that the experimental shear resistance values obtained were higher than the analytical values calculated based on flat web sections, an analysis that was made just for contrasting purposes. This suggests that web stiffeners provide a significant improvement in shear resistance.

However, the nominal shear strength values ( $V_n$ ) for the tested section will be calculated throughout the development of this dissertation. For this reason, the use of flat web purlins has been considered interesting in this study, as it will allow for a more detailed and accurate comparison between future experimental and analytical results.

Further numerical studies with the aid of the finite element method to simulate the test ensures a solid foundation for evaluating the structural behaviour of stiffened Z-purlins, contributing to the advancement of knowledge in the field and the development of more efficient and safer structural solutions.

## References

- [1] American Iron and Steel Institute (AISI), North American Specification for the Design of Cold-Formed Structural Members, AISI S100-16, Washington, DC, 2016.
- [2] Yu, W. W.; Laboube, R. A. and Chen, H. Cold-Formed Steel Design. 5<sup>a</sup> Edition. Hoboken: Wiley, 2020.
- [3] Pham, C. H. and Hancock, G. J. Numerical investigation of longitudinally stiffened web channels predominantly in shear, Thin-Walled Structures, Volume 86, 2015, Pages 47-55.
- [4] Sales, F.; Lima, A.; Pereira, E.; Veloso, L.; De Paula, J.; Silva, L.; Alencar, G. Análise teórica e experimental de terças Z com alma enrijecida com transpasse. Construmetal, São Paulo, 2023.
- [5] B.W. Schafer, S. Ádány, Buckling analysis of cold-formed steel members using CUFSM: conventional and constrained finite strip methods, in: Proceedings of the 18th International Specialty Conference on Cold-Formed Steel Structures, 2006, pp. 39–54.
- [6] R.A. LaBoube, W.W. Yu, Cold-formed steel web elements under combined bending and shear, in: Proceedings of the 4th International Specialty Conference on Cold-Formed Steel Structures, 1978, pp. 219–251.
- [7] C.H. Pham, G.J. Hancock, Experimental investigation of high-strength cold-formed C-sections in combined bending and shear, J Struct Eng Am Soc Civil Eng 136 (7) (2010) 866–878.
- [8] ASSOCIAÇÃO BRASILEIRA DE NORMAS TÉCNICAS. NBR 7008-3: Chapas e bobinas de aço revestidas com zinco ou liga de zinco-ferro pelo processo contínuo de imersão a quente - Parte 3: Aços estruturais Rio de Janeiro, p. 24. 2002.
- [9] American Society for Testing and Material (ASTM), Standard test method and definitions for mechanical testing of steel products, ASTM 370 (2017).
- [10] Silva, J. M. M. and Malite, M. Longitudinally stiffened web purlins under shear and bending moment, Thin-Walled Structures, Volume 148, 2020.